



Rational design of supramolecular self-assembly sensor for living cell imaging of HDAC1 and its application in high-throughput screening

Min Li^a, Huijuan Yu^{b,c}, Yiran Li^a, Xin Li^a, Shiqing Huang^e, Xiaogang Liu^e, Gaoqi Weng^a, Lei Xu^f, Tingjun Hou^a, Dong-Sheng Guo^{b,**}, Yi Wang^{a,c,d,*}

^a College of Pharmaceutical Sciences, Zhejiang University, Hangzhou 310058, China

^b College of Chemistry, Key Laboratory of Functional Polymer Materials (Ministry of Education), State Key Laboratory of Elemento-Organic Chemistry, Tianjin Key Laboratory of Biosensing and Molecular Recognition, Nankai University, Tianjin 300071, China

^c State Key Laboratory of Component-based Chinese Medicine, Tianjin Key Laboratory of TCM Chemistry and Analysis, Tianjin University of Traditional Chinese Medicine, Tianjin 301617, China

^d Future Health Laboratory Innovation Center of Yangtze River Delta Zhejiang University, Jiaxing 314100, China

^e Fluorescence Research Group, Singapore University of Technology and Design, 8 Somapah Road 487372, Singapore

^f Institute of Bioinformatics and Medical Engineering, School of Electrical and Information Engineering, Jiangsu University of Technology, Changzhou 213001, China



ARTICLE INFO

Keywords:

Host-guest chemistry
Supramolecular tandem assay
Histone deacetylase 1
Inhibitor screening

ABSTRACT

Supramolecular chemistry offers new insights in bioimaging, but specific tracking of enzyme in living cells via supramolecular host-guest reporter pair remains challenging, largely due to the interference caused by the complex cellular environment on the binding between analytes and hosts. Here, by exploiting the principle of supramolecular tandem assay (STA) and the classic host-guest reporter pair (*p*-sulfonatocalix[4]arene (SC4A) and lucigenin (LCG)) and rationally designing artificial peptide library to screen sequence with high affinity of the target enzyme, we developed a “turn-on” fluorescent sensing system for intracellular imaging of histone deacetylase 1 (HDAC1), which is a potential therapeutic target for various diseases, including cancer, neurological, and cardiovascular diseases. Based on computational simulations and experimental validations, we verified that the deacetylated peptide by HDAC1 competed LCG, freeing it from the SC4A causing fluorescence increase. Enzyme kinetics experiments were further conducted to prove that this assay could detect HDAC1 specifically with high sensitivity (the LOD value is 0.015 µg/mL, ten times lower than the published method). This system was further applied for high-throughput screening of HDAC1 inhibitors over a natural compound library containing 147 compounds, resulting in the identification of a novel HDAC1 down-regulator (Ginsenoside RK3). Our results demonstrated the sensitivity and robustness of the assay system towards HDAC1. It should serve as a valuable tool for biochemical studies and drug screening.

1. Introduction

Post-translational modification (PTM) is an important modality to regulate protein functions in biological systems. ϵ -Amino acetylation of lysine residues in proteins is a PTM that impacts DNA transcription, replication, and protein-protein interactions by modifying protein structure (Falkenberg and Johnstone, 2014). This PTM pattern is mainly regulated by histone deacetylases (HDACs) and histone acetyltransferases (HATs). Till now, 18 human HDACs have been identified and divided into four classes based on their sequence homology (McClure et al., 2018). Class I HDACs, particularly HDACs 1, 2 and 3, are

overexpressed in tumors and play crucial roles in regulating gene expression related to carcinogenesis (Arrowsmith et al., 2012). Among them, HDAC1 also abnormally upregulated in various other diseases, such as neurological disorders, immune disorders (Falkenberg and Johnstone, 2014) and cardiovascular diseases (Herr et al., 2018; Li et al., 2020). Activity tracking assays are vital for studying biological mechanisms, enzymatic deacetylation regulation and screening novel HDAC1-targeting inhibitors from compound libraries, which is crucial in the fields of biology, medicine and pharmacy. Fluorescent sensors are ideal for enzyme activity tracking due to their high sensitivity, non-destructive measurement and imaging capabilities, surpassing

* Corresponding author. College of Pharmaceutical Sciences, Zhejiang University, Hangzhou 310058, China.

** Corresponding author.

E-mail address: zjuwangyi@zju.edu.cn (Y. Wang).

other biochemical methods like radioisotopes, antibodies, HPLC, mass spectrometry and electrochemical analyzers (Hu et al., 2020; Moreno-Yruela et al., 2021; Wang et al., 2017). Up to date, a lot of fluorescent sensors have been developed for HDACs (Tan and Li, 2022; Tang et al., 2022), but few realized HDACs imaging with selectivity for HDAC isoforms (Liu et al., 2018, 2022). Zhang et al. reported a fluorescent probe with great selectivity towards Class I HDACs (Zhang et al., 2021), but it may result in background fluorescence from non-specifically bound or excessive probes and precluding real-time intracellular HDAC activity detection because it was designed by tagging a fluorophore to HDAC-isoform selective inhibitors. Furthermore, the cumbersome synthesis of these probes limits their widespread use. Till now, there is no fluorescent sensors has been designed for imaging of HDAC1 in living cells. Developing selective HDAC1 fluorescent biosensor for high-throughput screening and live cell imaging still remains a great challenging.

The design of substrates with high affinity and selectivity for HDAC1 is the basis for achieving selective detection of HDAC1. As a protein modification enzyme, the natural substrate of HDAC1 is proteins with ε-Amino acetylation of lysine residues. Peptides, as amino acid oligomers with the same building blocks as proteins, can potentially replace proteins. Peptides also have higher stability and are easier to synthesize and modify than proteins, making them very suitable as enzyme-specific substrates for designing enzyme sensors (Liu et al., 2015). Specific peptide sequences with high affinity for HDAC1 can be obtained by optimizing and screening artificial peptide libraries. Researches on constructing fluorescent enzyme sensors using peptide substrates (Placzek et al., 2010; Wang et al., 2015; Yang et al., 2020) often employs the covalent linking method to conjugate the peptide substrate with a signal marker, which often involves complex synthesis, purification and structure identification processes. Supramolecular tandem assay (STA) based on the principles of supramolecular chemistry (Hennig et al., 2007) provides a label-free strategy for using peptides as enzyme recognition component and then achieving fluorescence signal transformation. STA utilizes fluorescent dyes for sensitive and convenient signal transduction, introduces enzymes to achieve specific recognition of analytes, and employs macrocycles to distinguish enzymatic reaction substrates and products (Umali and Anslyn, 2010), enabling real-time monitoring of enzymatic reactions because of the dissociation or binding of the macrocyclic host and guest running much faster than enzymatic reaction (Nau et al., 2009). Till now, many enzyme assays based on host-guest interaction have been established (Nilam and Hennig, 2022), but examples of intracellular enzyme imaging based on STA are still rare because of the following reasons: 1) Incomplete complexation of the reporter pair may induce background noise (You et al., 2015) and some established STA systems even exhibit “switch-off” fluorescence change after enzymatic reaction (Liu et al., 2019; Yue et al., 2019; Zhao et al., 2020). 2) The complex cellular environment may interfere with the binding between the target analyte, such as enzyme products, and the host, thus affecting the transduction of the fluorescence signal. Therefore, implementing the STA strategy in the cellular environment, may need 1) select a reporter pair with high-affinity, which do not exhibit fluorescence enhancement in the presence of substrate alone, and show strong fluorescence enhancement when introduced enzymes; 2) optimize the selectivity of the substrate for the enzyme and the affinity differences between substrate/product for the artificial host.

In our manuscript, we first rationally constructed a peptide library for optimizing high-affinity peptide candidates of HDAC1. Based on the structural characteristics of the peptide sequence after deacetylation by HDAC1, we selected SC4A as a supramolecular host because it can form complexes with cationic amino acids (Arena et al., 2006) and peptides (McGovern et al., 2014). LCG was then selected as indicator due to its high quantum yield and strong affinity to SC4A, showing significant fluorescence quenching upon complexation with SC4A (Guo et al., 2011). Afterwards, the candidate peptides were screened to obtain the sequence with sufficiently high affinity for SC4A and sufficiently low

affinity between its corresponding acetylated peptide and SC4A, ultimately constructing a product-selective “switch-on” STA sensor suitable for selective imaging of HDAC1 in living cells. As shown in Scheme 1, SC4A encapsulated LCG is non-emissive even in the presence of Ac-peptide due to photo-induced electron transfer (PET). HDAC1 catalyzed the deacetylation of the weak competitor Ac-peptide to continuously form a strong competitor peptide displacing LCG from SC4A, which results in a significant increase in fluorescence intensity. Moreover, this approach is effectively applied to living cells. Specifically, this sensor was incubated with cells, causing endogenous HDAC1 deacetylate substrates and produce products displacing LCG from SC4A. It also displays great potential in the high throughput screening of HDAC inhibitors.

2. Experimental section

2.1. Optimization of Ac-peptides binding to LCG-SC4A supramolecular system

500 μM Ac-peptides were incubated with 50 μg/mL HDAC1 in 10 mM HEPES buffer (pH = 8.0) at 37 °C for 2 h. The samples and standard samples (Ac-peptides and peptides) were then analyzed by HPLC. Deacetylation rate of each Ac-peptide was calculated using the following equation:

$$\text{Deacetylation rate (\%)} = [(P_0 - P_S) / P_0] \times 100\%$$

(P_0 : the peak area of Ac-peptide before deacetylation; P_S : the peak area of Ac-peptide after deacetylation).

Then competitive titrations were performed in HEPES buffer (10 mM, pH 8.0) at room temperature to determine the association constant (K_a) between SC4A and peptides. The direct fluorescence data from the competitive titrations were fitted in a nonlinear manner (<http://www.jacobs-university.de/ses/wnau>).

2.2. Fluorescence measurement

To optimize assay conditions, HDAC1 (0.5 μg/mL) and LCG/SC4A (2 μM/4 μM) were first incubated with Ac-peptide 14 (50 μM) in HEPES buffer with different concentrations, then incubated with Ac-peptide 14 (50 μM) in 5 mM HEPES of different pH value, and then incubated with different concentrations of Ac-peptide 14 in 5 mM HEPES buffer, pH 8.0.

To test the sensitivity of this assay, 2 μM/4 μM LCG/SC4A and 50 μM Ac-peptide 14 was incubated with different concentrations of HDAC1, recording fluorescent intensity at the interval of 120 s until the fluorescence intensity approximately stable.

To determine the K_m value of Ac-peptide 14 towards HDAC1, 2 μM/4 μM LCG/SC4A and 0.5 μg/mL HDAC1 was incubated with different concentrations of Ac-peptide 14, recording fluorescent intensity at the interval of 120 s until the fluorescence intensity approximately stable.

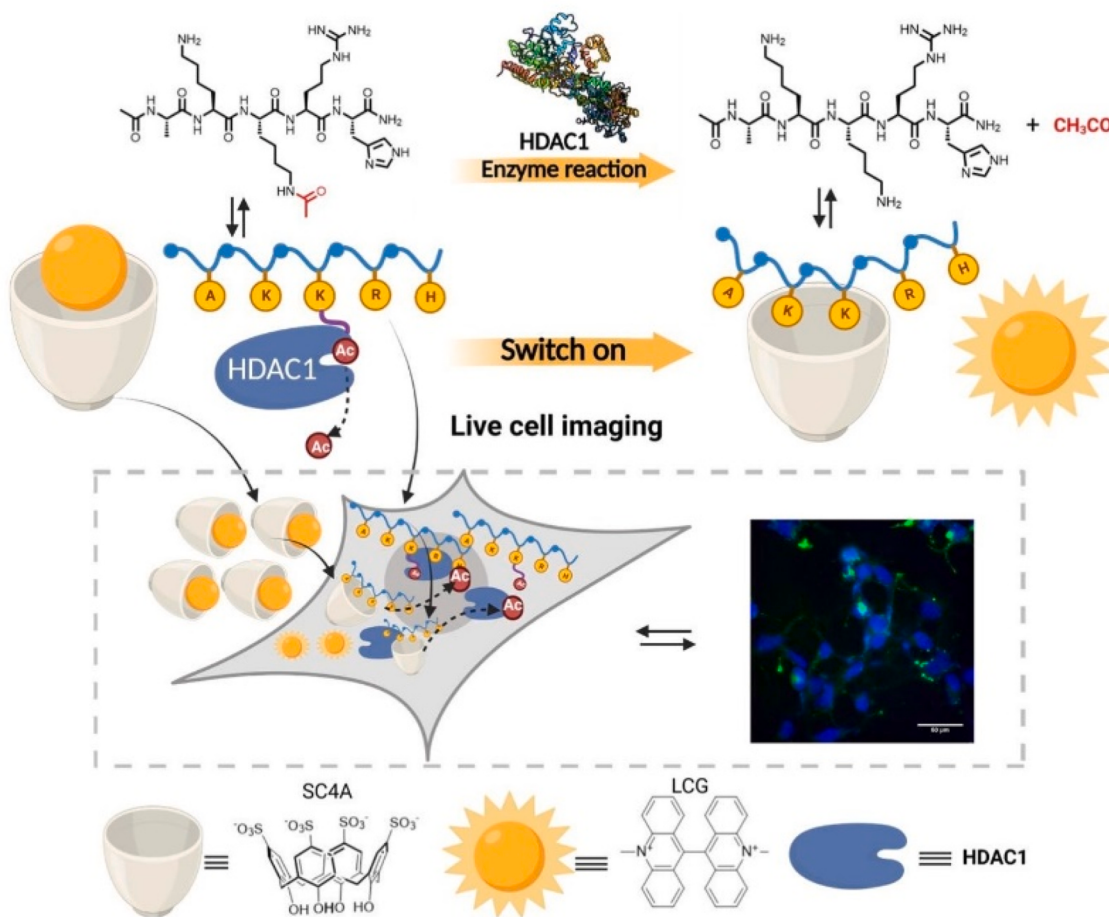
To determine the IC_{50} value of HDAC inhibitors, HDAC1 and this sensor were incubated with different concentration of Vorinostat (SAHA) and Entinostat (MS-275).

To test the detection selectivity, this sensor was also incubated with other macromolecules (50 μg/mL) and histone deacetylases (5 μg/mL), and the fluorescence measurements were taken after 3 h incubation.

All the fluorescence intensity was recorded by TECAN infinite M1000 Multi-function microplate reader ($\lambda_{ex} = 368$ nm, $\lambda_{em} = 505$ nm) after incubation for 3 h at 37 °C.

2.3. Living cell imaging with Ac-peptide based supramolecular sensor

All cell imaging experiments were carried out on ImageXpress® Micro Confocal system (Molecular Devices). Cells were seeded in 96-well black plate with clear bottom (Greiner 655,090) at an appropriate density and allowed to attach to the plate for 12 h in growth



Scheme 1. Schematic of LCG-SC4A-Ac-peptide sensor. Acetylated peptide can be deacetylated by HDAC1 and then triggered the competitive displacement process causing fluorescent responses.

medium at 37 °C with 5% CO₂. All wells were divided into three groups and reagents were added as shown below: 1) LCG 25 μM, 2) LCG/SC4A 25/250 μM and 3) LCG/SC4A/Ac-peptide14 25/250/300 μM. Fluorescence images were taken by ImageXpress Micro Confocal system (Molecular devices) after 3 h incubation with nine images acquired from each independent well for fluorescent intensity analysis. Excitation and emission wavelength:488 nm and 525 nm for LCG; 405 nm and 450 nm for Hoechst. The fluorescence intensity was calculated with MetaXpress PowerCore software (Molecular devices).

2.4. High-throughput screening method

The HEK293T cells were seeded in 96-well black plates with clear bottom at a density of 8000/well. After the cells adhered to the plate for 12 h, compounds were pre-administered for 12 h. The old culture medium was then removed and stained with LCG/SC4A/Ac-peptide 14 (25/250/300 μM). The cell fluorescent images were obtained and analyzed with the same methods mentioned in the living cell imaging section. The inhibition rate of drugs on HDAC1 was calculated by $[(I_0 - D)/I_0] \times 100\%$ (I_0 : the average fluorescence intensity of green fluorescence per cell in control group; D : the average fluorescence intensity of green fluorescence per cell in administration group).

3. Results and discussion

3.1. Rationally design of Ac-peptide-based supramolecular sensor for HDAC1 detection

In this work, in order to realize HDAC1 selectivity, a candidate library of 175 Acetylated-lysine-centered 5-mer peptides were first constructed for substrate peptide screening by knowledge- and mechanism-based design (Fig. 1A), which is composed of deacetylation sites regulated by HDAC1 as reported previously (Li et al., 2014; Nalawansha and Pflum, 2017; Wang et al., 2019; Wu et al., 2021) and the highly-correlated amino acids with lysine acetylation at four randomized positions (Schwartz et al., 2009) to screened peptide candidates with high affinity of HDAC1. As mentioned in Section 1, the complexation-induced quenching reporter pair, SC4A-LCG, which was applied for monitoring cellular uptake of specific analytes (Nguyen and Anslyn, 2006), has been selected for established STA sensor. To employ STA sensing HDAC1 in living cells, we also need: 1) minimize the interference of other cellular substances on the complexation between the product and the host; 2) lower the fluorescence as much as possible when HDAC1 was inhibited or knock down in live cells. Therefore, the candidate sequences need to be further optimized to achieve sufficiently high affinity between the peptide and SC4A and sufficiently low affinity between the corresponding acetylated-peptide and SC4A.

First, instead of measuring the deacetylation rates of all 175 acetylated peptides one by one, we randomly selected 14 acetylated peptides (Ac-peptides) to test their deacetylation rates of HDAC1 by HPLC methods. Five Ac-peptides (Ac-peptide11,7,5,12 and 14) showed more

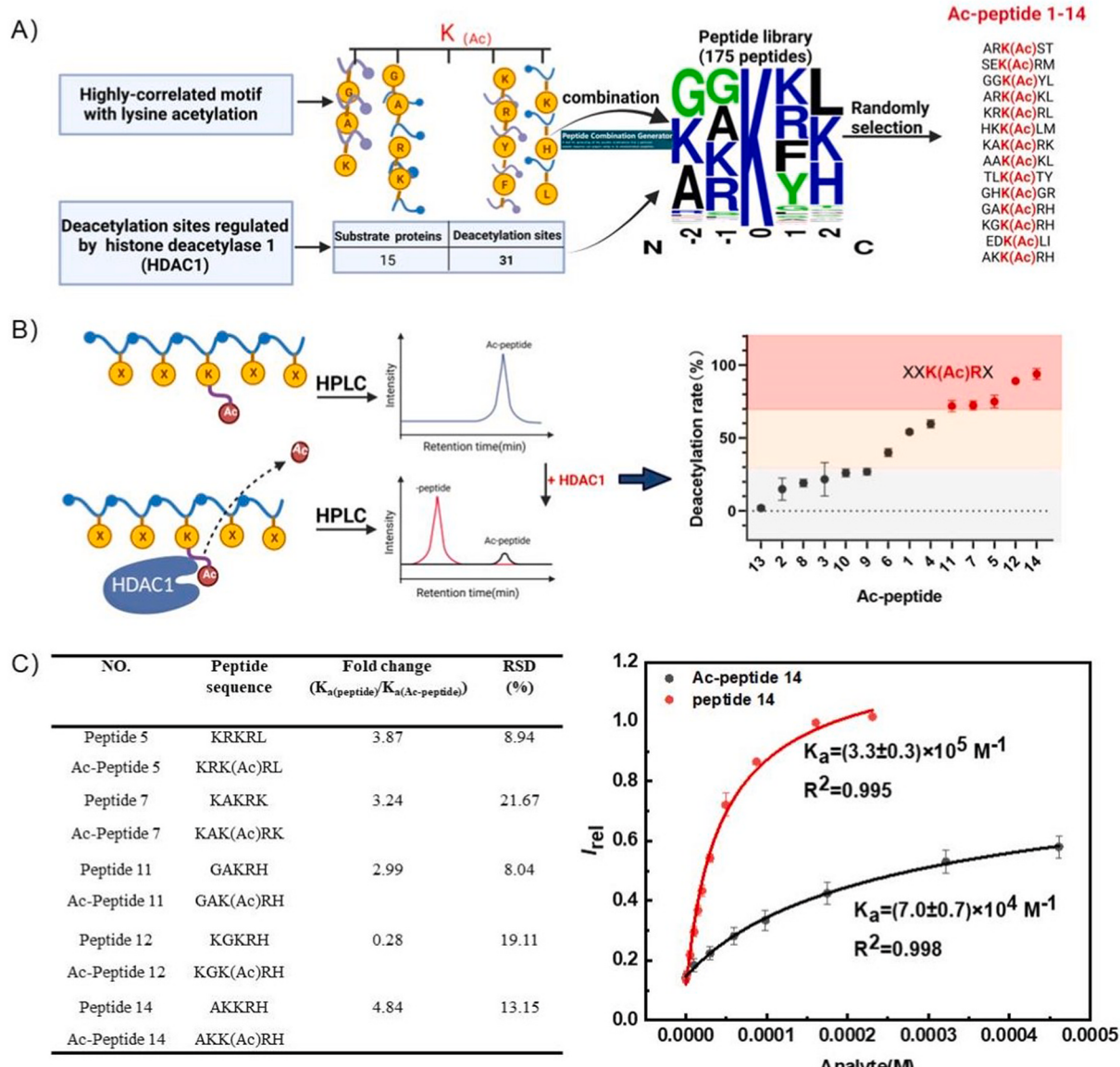


Fig. 1. The most suitable Ac-peptide screening for HDAC1 detection using host-guest strategy. (A) The pipeline of acetylated peptide library construction. (B) Detection of HDAC1 deacetylation rate towards the selected Ac-peptides. $n = 3$. (C) Fold change of Association constants (K_a) values for the complexation of SC4A with peptides and corresponding Ac-peptides in 10 mM HEPES, pH 8.0, $n = 6$. Data are presented as mean \pm SEM.

than 70% efficacy when incubated with HDAC1 (Fig. 1B). Analysis of the structure-activity relationship revealed that topological polarity surface area (TPSA) (Pearson correlation coefficient = 0.6173) contributed significantly to the deacetylation capability (Fig. S15). Molecular docking showed that the Ac-peptide 14 with the highest affinity of HDAC1 occupied the enzyme active site by the key interactions of several hydrogen bond between this peptide and the residues of Gln-26, Asp-99, Gly-149, Asn-95. Moreover, the lysine to the right of the acetylation site in Ac-peptide 14 is inserted into another cavity at the rim of the active site further enhancing the binding affinities (Fig. S16), which indicated that the binding affinity between other amino residues in Ac-peptides and HDAC1 could crucially affect the catalytic efficiency because the central-acetylated-lysine remained unchanged.

The association constant (K_a) between SC4A and LCG was in consistent with previous study (Guo et al., 2011), which fitted as $(4.6 \pm 0.4) \times 10^6 \text{ M}^{-1}$ in 10 mM HEPES at pH = 8.0 (Fig. S17 B). To obtain a pair of peptides (Ac-peptide and its product peptide) from 5 pairs of candidate peptides with the largest binding difference to SC4A,

competitive titrations were performed to determine the K_a values between these candidate peptides and SC4A, which were used to quantify the binding affinity between analytes and macrocyclic receptors. The fold changes of K_a values between peptides and their corresponding Ac-peptides were subsequently calculated to demonstrate the disparity in binding affinities between substrates and products to the supramolecular host (Fig. 1C). Finally, Ac-peptide 14 was selected as the substrate to develop a STA assay for HDAC1 detection, for its highest deacetylation rate of HDAC1, sufficiently high affinity of its product for SC4A and the largest contrast in the binding of this peptide and its product to SC4A.

Given the results of substrate optimization, we next performed experiment to verify the accessibility of this sensor to HDAC1. As shown in Fig. 2A, the addition of HDAC1 to LCG/SC4A system caused only a little fluorescence recovery. This implies that the enzyme itself does not interfere with the reporter pair, thus eliminating the need for additional processing steps in the actual detection process, unlike previous studies (Yu et al., 2021). However, the addition of HDAC1 to

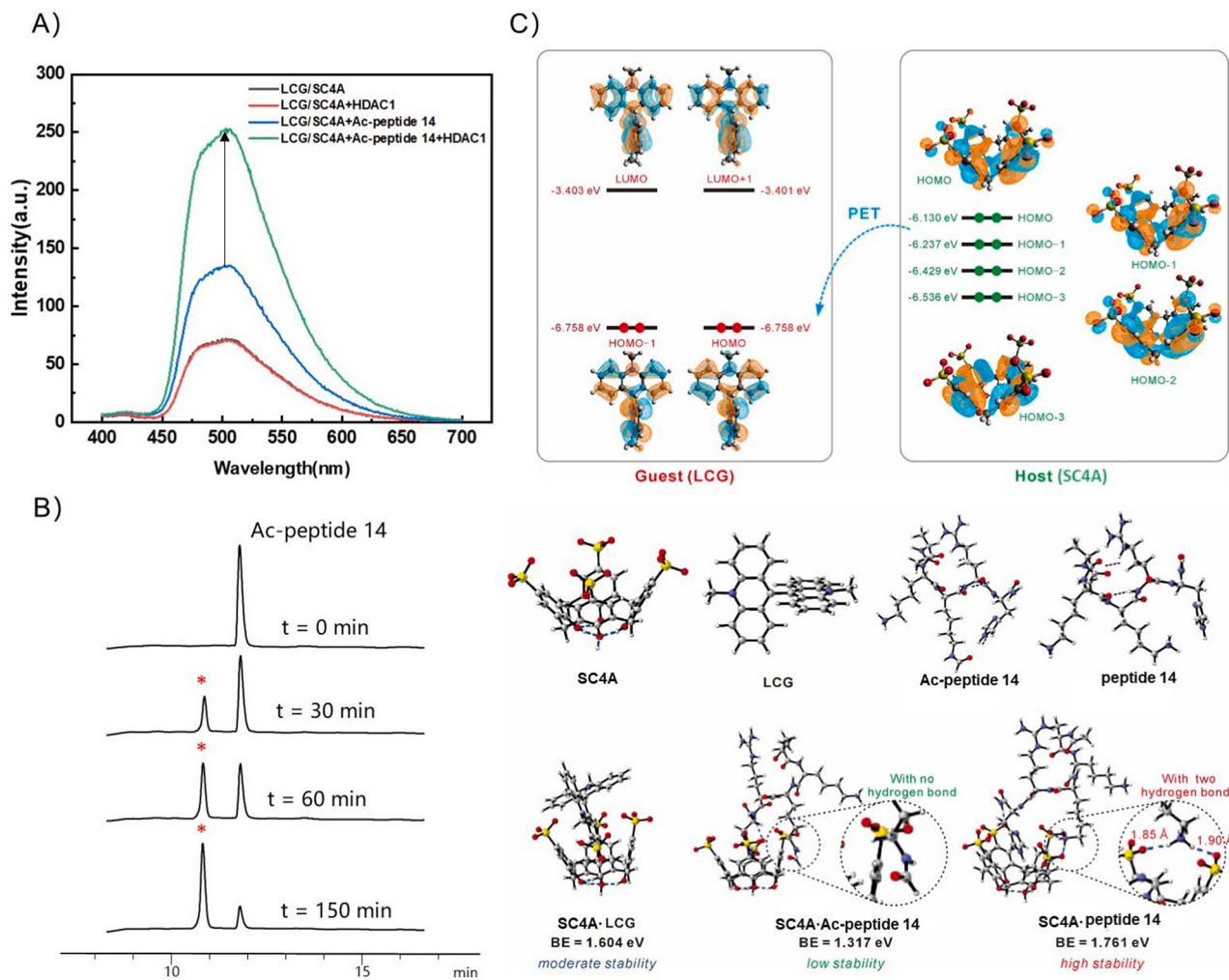


Fig. 2. HDAC1 triggered LCG displacing from SC4A. (A) Fluorescence spectra of 50 μ M Ac-peptide 14 incubated with 5 μ g/mL HDAC1 and LCG/SC4A (2/4 μ M) in 10 mM HEPES, pH 8.0, 37 °C, 3 h, n = 6. (B) HPLC monitoring of the deacetylation reactions of Ac-peptide 14 (2 mM) in the presence of 16.67 μ g/mL HDAC1 in 5 mM HEPES buffer, pH 8.0, 37 °C, *denotes the newly formed product. (C) The fluorescence quenching mechanism of LCG when binding to SC4A and the optimized structures of the complex of host (SC4A) and three guest molecules (LCG, Ac-peptide 14, peptide 14).

LCG/SC4A/Ac-peptide 14 system caused a significant fluorescence enhancement, indicating HDAC1 triggered LCG displacing from SC4A. HPLC results also confirmed the enzymatic response of Ac-peptide 14 under this condition, which showed more than half of Ac-peptide 14 was deacetylated after co-incubation with HDAC1 for 60 min at this condition (Fig. 2B).

Computational simulations were performed to further confirm the feasibility of this sensor in detecting HDAC1. Firstly, LCG was quenched due to photo-induced electron transfer (PET) when binding to SC4A. As shown in Fig. 2C, the photoexcitation/de-excitation process from S0 to S1 is primarily controlled by transitions from HOMO/HOMO-1 to LUMO/LUMO+1 in LCG monomers and the HOMO/HOMO-1 (-6.758 eV) and LUMO/LUMO-1 (approximately -3.4 eV) orbitals are degenerate due to the symmetrical structure of LCG. These frontier molecular orbitals exhibit conjugation throughout the entire fluorophore, facilitating $\pi-\pi^*$ transitions that result in bright fluorescence in LCG monomers. Several occupied molecular orbitals of SC4A are positioned between the HOMO and LUMO levels of LCG. The energy levels of these frontier molecular orbitals are consistent with the photo-induced electron transfer (PET) mechanism (Biedermann and Schneider, 2016) (Fig. 2C). Based on this fluorescence quenching mechanism, then the results of binding energy(BE) calculations followed the increasing order of SC4A-Ac-peptide14 (1.317 eV) < SC4A-LCG (1.604 eV) < SC4A-peptide14 (1.761 eV). The amide group in Ac-peptide 14 was

transformed into an ammonium group (which is protonated under physiological pH conditions) with the HDAC enzyme, form two additional hydrogen bond donating sites in this ammonium group, which greatly enhance the stability of SC4A-peptide14. Owing to this large BE, peptide 14 could thus effectively displace LCG from SC4A and then realized HDAC1 tracking.

3.2. The sensitivity and specificity of Ac-peptide-based supramolecular sensor towards HDAC1

Considering that the above results demonstrated the feasibility of the sensor for sensing HDAC1, we further investigated the sensitivity and selectivity of this assay. According to previous studies (Yue et al., 2019; Zheng et al., 2021), the enzymatic reaction rate is directly proportional to the enzyme concentration when the substrate is in excess. Therefore, we co-incubated different concentrations of HDAC1 with LCG/SC4A/Ac-peptide14 and recorded the fluorescence intensity over time to determine the initial velocity of the enzyme reaction by calculating the slope of the enzyme kinetics curve, which was further used to calculate the limit of detection (LOD) value. This sensing assay worked as expected with the fluorescence intensity of the sensing system gradually increasing during 3 h in the presence of various HDAC1 concentrations (Fig. 3A) and the LOD value was calculated as 0.015 μ g/mL (Fig. 3B) according to the function(LOD = 3.3 δ/S) mentioned in

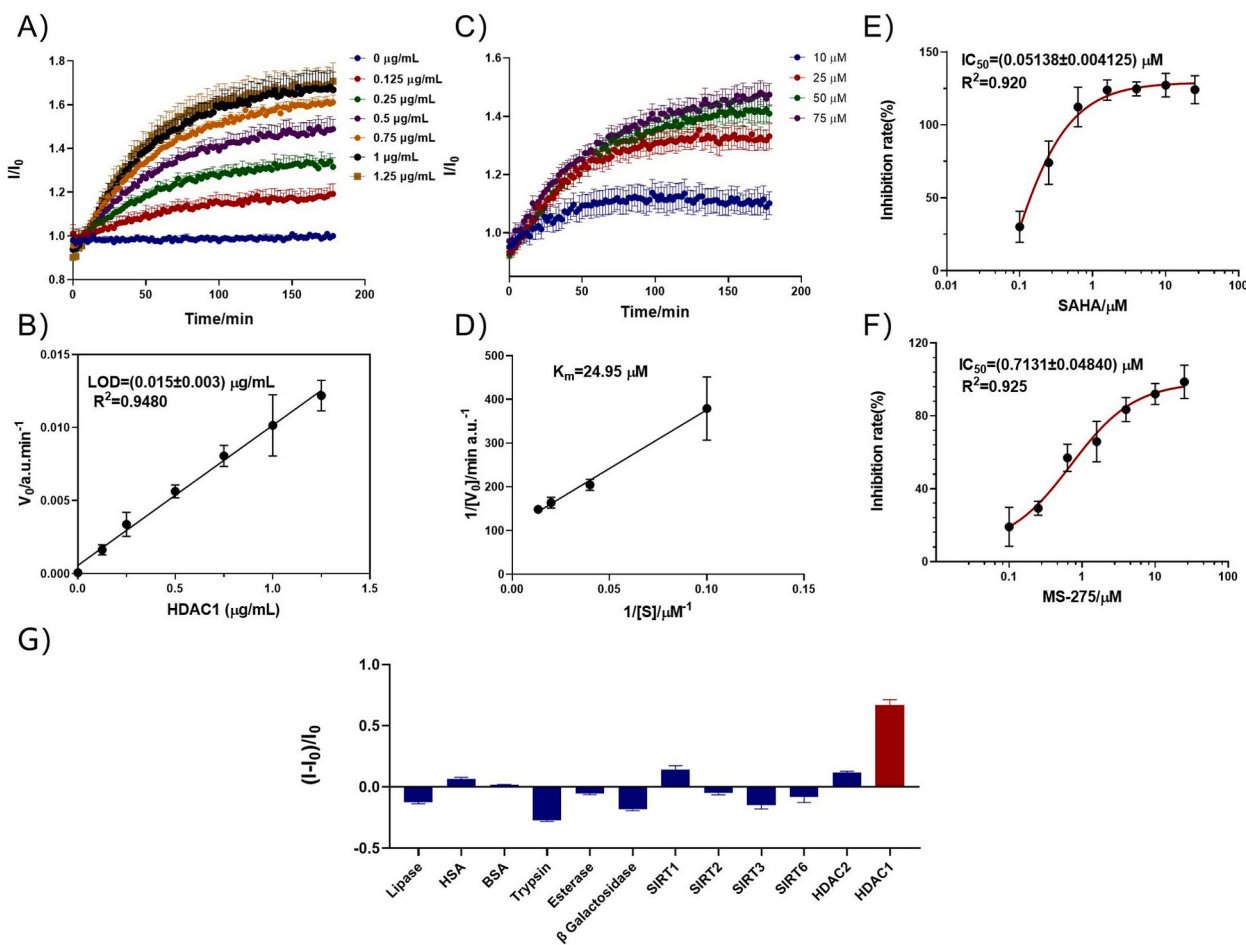


Fig. 3. Properties of LCG-SC4A-Ac-peptide 14 assay towards HDAC1. (A) The fluorescence response increased with HDAC1 concentration ranging from 0 to 1.25 $\mu\text{g/mL}$. I represents fluorescence intensity of samples with different concentration of HDAC1, I_0 represents fluorescence intensity of the blank sample (the concentration of HDAC1 is 0) at the same time. (B) Linear relationship between the initial rates of the enzymatic reaction and the enzyme concentrations. (C) Continuous fluorescence response for HDAC1 (0.5 $\mu\text{g/mL}$) and LCG/SC4A (2/4 μM) incubated with different concentrations of Ac-peptide 14, $n = 3$. (D) The Lineweaver-Burk plot for HDAC1. (E) and (F) Dose-dependent inhibition of SAHA and MS-275, $n = 6$. (G) Fluorescence response of LCG/SC4A/Ac-peptide 14 system to different HDACs (5 $\mu\text{g}/\text{mL}$) and other analytes (50 $\mu\text{g}/\text{mL}$) after incubation at 37°C for 3 h., $n = 6$. I : fluorescence intensity of samples with different analytes, I_0 : fluorescence intensity of the blank sample (without analytes). Data are presented as mean \pm SEM.

previous study (Zhao et al., 2020). It's much lower than the LOD value of a near-infrared (NIR) fluorescent probe published before, which is 2.93 nM equivalent to 0.208 $\mu\text{g/mL}$ (Shu et al., 2022). A further investigation revealed that the K_m value was 24.95 μM for the Ac-peptide 14 toward HDAC1 (Fig. 3C and D) and is much lower than that 152.61 μM of HDAC2 (Fig. S21), which has high homology with HDAC1 (Krämer, 2023). Furthermore, the feasibility of this sensing system in screening inhibitors was confirmed by determining the IC_{50} value of pan-inhibitor Vorinostat (SAHA) and specific HDAC1/HDAC3 inhibitor Entinostat (MS-275) (Fig. 3E and F). The IC_{50} values were respectively measured as 0.05138 and 0.7131 μM , close to the values reported in the literatures (Choi et al., 2019; Singh et al., 2021). The sensor also demonstrated excellent selectivity towards HDAC1 compared with other biological macromolecules and enzymes (Fig. 3G). All these results confirmed this sensor could precisely sense HDAC1 and facilitate inhibitor screening *in vitro*.

3.3. Ac-peptide-based supramolecular-sensor enabled sensing HDAC1 activity in living cells

We further applied the sensor for tracking HDAC1 in the HEK293T cells. The negligible cytotoxicity of LCG, SC4A, and Ac-peptide 14 was first verified (Fig. S23). Strong fluorescence signals were observed

when the HEK293T cells were only treated with LCG, indicating that HEK293T cells can uptake LCG. In contrast, HEK293T cells remained dark when co-incubated with LCG and 10 \times SC4A (Fig. S24). These results indicated SC4A quenching fluorescence of LCG in living cells. After co-incubating LCG/SC4A and the Ac-peptide 14 with the HEK293T cells, a bright fluorescence was observed, indicating the displacement of LCG from SC4A inside cells (Fig. 4A). To further confirm that the displacement of LCG from SC4A was triggered by HDAC1, we performed cell inhibition study with MS-275. An approximate 2-fold decrease of fluorescence intensity is observed for MS275-treated cells compared with normal cells (Fig. 4A and S25), suggesting that HDAC1 could trigger Ac-peptide 14 deacetylation into peptide 14, thus displacing LCG from SC4A. This sensor was also applied in the H9c2 and the Hela cells (Fig. S26). Furthermore, siRNA knockdown experiments with HEK293T cells showed that fluorescence diminished when HDAC1 was knocked down (Fig. 4B). All of the above results strongly demonstrated the sensing assay enables intracellular HDAC1 imaging.

3.4. Ac-peptide based-supramolecular sensor facilitated the high-throughput screening for HDAC inhibitors in living cell imaging manner

Inhibition of HDACs has demonstrated therapeutic potential in diseases including cancer, neurological diseases, immune diseases, and

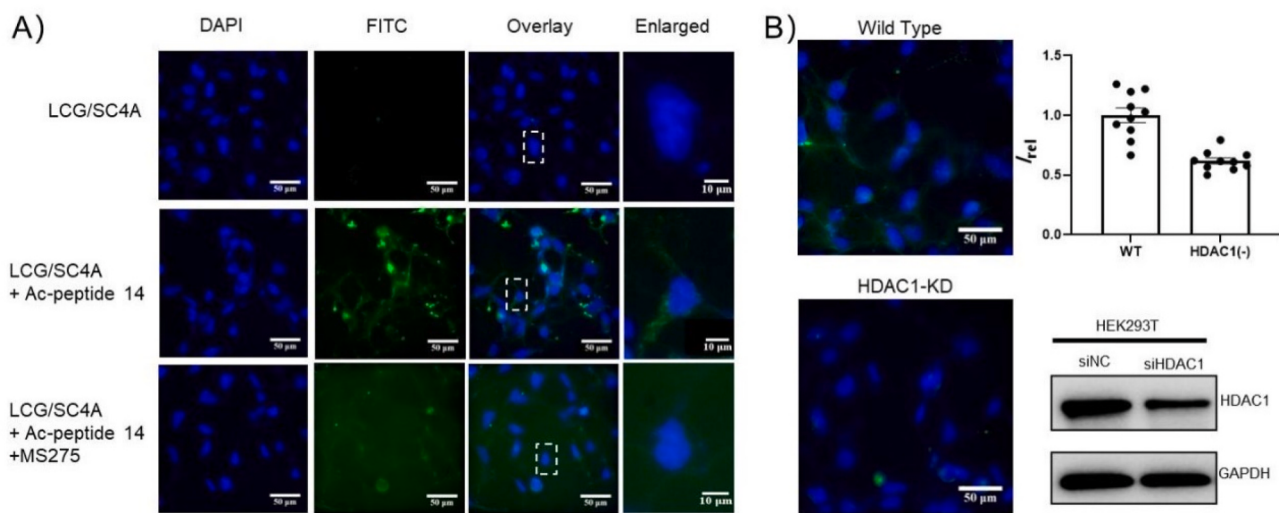


Fig. 4. Intro-cellular HDAC1 triggered Ac-peptide deacetylation and then displacing LCG from SC4A. (A) Fluorescence microscopy images of HEK293T cells incubated with the LCG/SC4A/Ac-peptide 14. Representative images are shown from $n = 6$ independent wells. Scale bar: 50 μ m and 10 μ m. (B) Fluorescence microscopy image of wild-type HEK293T cells and HDAC1-knock down HEK293T cells incubated with this sensor. Representative images and the statistically quantified data on the cellular fluorescence intensity are shown from $n = 10$ independent wells, all the data are normalized to the control group and presented as mean \pm SEM. Additionally, the western blotting demonstrated the protein level of HDAC1 after conducting siRNA knockdown experiments in HEK293T cells.

cardiovascular diseases. While some HDAC inhibitors like Vorinostat, Romidepsin, and Belinostat have been approved for treating certain types of lymphoma (Duvic et al., 2007; Molife and de Bono, 2011; VanderMolen et al., 2011), their lack of specific inhibitory effects may lead to unpredictable side effects. As a result, the search for lead compounds specifically targeting histone deacetylase isoforms has gained momentum. Natural product libraries are considered valuable resources for screening potential lead compounds.

A high-throughput screening pipeline in HDAC1 inhibitor screening over a natural product library containing 147 compounds using ImageXpress® Micro Confocal system (Molecular Devices) was constructed with this Ac-peptide-based supramolecular sensor. Most of the compounds exhibited weak or no inhibitory effects of HDAC1 (Table S3 and Fig. 5B). Five of the top 11 compounds with high inhibitory activity, i.e. Honokiol (Singh et al., 2013), 20(S)-Ginsenoside CK (Kang et al., 2013), Chrysophanol (Lu et al., 2017), Emodin (Ha et al., 2011) and Luteolin (Attoub et al., 2011) have been previously reported to down-regulated HDAC1 protein levels or inhibit HDAC activity (Table S2). Among the unreported hits, Salvianic acid A (SAA) could significantly inhibit HDAC1 activity (Fig. S27), while protocatechuic acid (PCA) and Ginsenoside Rk3 could significantly down-regulated cellular protein level (Fig. 5C). However, it is crucial to identify pan-assay interference compounds (PAINS) in high throughput screening (Baell and Walters, 2014), as some hits could nonspecifically bind to multiple proteins and interfere the screening results. Among our hits, emodin and chrysophanol are quinone, while Luteolin, protocatechuic acid and Salvianic acid A are catechol, which may act as covalent modifier, redox cycler, or metal complexer resulting in false positive outcomes. We verified whether the unreported PCA and SAA are PAINS by assessing binding directly with Cellular Thermal Shift Assay (CETSA). As shown in Fig. S29, they couldn't protect HDAC1 protein from temperature-dependent degradation in temperature- and dose-dependent CETSA assays, indicating their inhibitory effect does not depend on a specific, drug-like interaction between the molecule and the protein. Whereas CETSA assays showed Ginsenoside Rk3 could bind HDAC1 directly and down-regulated protein level (Fig. 5D and E). As shown in Fig. S30, the mRNA level and protein degradation results further indicated that Ginsenoside Rk3 may down-regulate protein levels by increasing protein degradation.

4. Conclusions

In conclusion, by exploiting supramolecular tandem assay and the LCG-SC4A reporter pair and rationally screening for high-affinity acetylated peptide of HDAC1, we have developed a novel and straightforward label-free sensing system (LCG-SC4A reporter pair and Ac-peptide 14(AKK(Ac)RH)). Based on computational simulation and experimental verification, we demonstrated that the proposed system enables specifically detect HDAC1 with high sensitivity in and outside live cells, offering advantages such as simplicity and avoidance of complex synthesis. We successfully conducted a high-throughput screening of HDAC inhibitors over a natural compounds library comprising 147 compounds by exploiting a high-content imaging system, identified a novel HDAC1 down-regulator (Ginsenoside RK3), indicating its great potential in drug screening. For the present assay, there is still a distance from spatially locating HDACs in live cells and realizing imaging HDACs *in vivo*. Future work could include integrating the STA sensing system with other strategies such as nano aggregates and rotaxane to enhance binding efficiency, minimize interference in more complex environments and realize spatially locating HDACs *in vivo*.

CRediT authorship contribution statement

Min Li: Methodology, Formal analysis, Investigation, Writing – original draft. **Huijuan Yu:** Methodology. **Yiran Li:** Formal analysis. **Xin Li:** Writing – review & editing. **Shiqing Huang:** Formal analysis, Software. **Xiaogang Liu:** Writing – review & editing. **Gaoqi Weng:** Formal analysis, Software. **Lei Xu:** Software. **Tingjun Hou:** Writing – review & editing. **Dong-Sheng Guo:** Writing – review & editing. **Yi Wang:** Supervision, Funding acquisition, Project administration, Conceptualization, Writing – review & editing.

Declaration of competing interest

The authors declare that they have no known competing financial interests or personal relationships that could have appeared to influence the work reported in this paper.

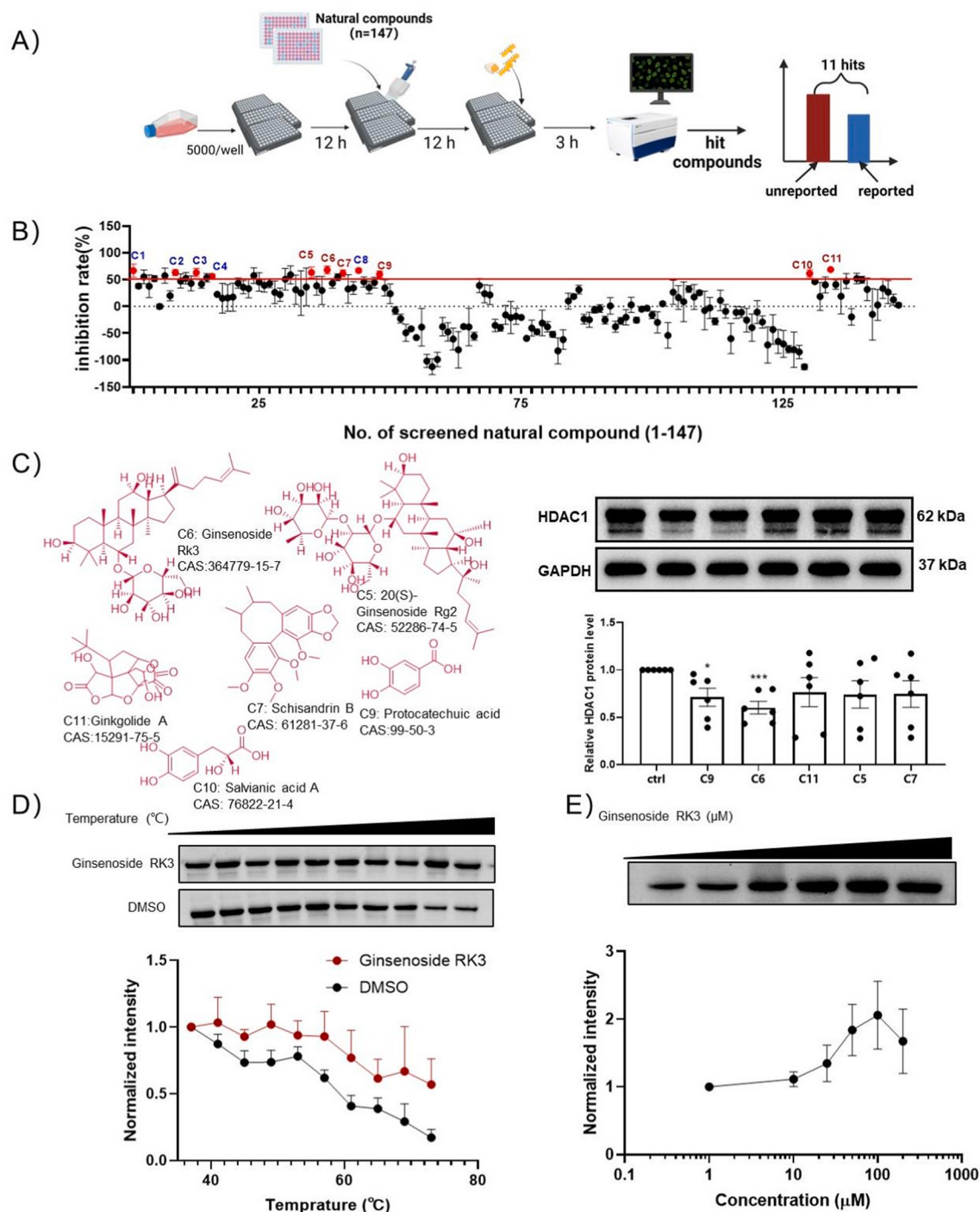


Fig. 5. HDAC inhibitor screening with LCG-SC4A-Ac-peptide 14 assay using live cell imaging. (A) The illustration of high-throughput screening workflow. (B) Screening results, n = 3. (C) The molecular structures of unreported hit compounds and the Western blot results of HDAC1 in HEK293T cells preincubated with them, data are analyzed using unpaired two-tailed t-test, *means p < 0.05 and ***means p < 0.001 compared with the control group, n = 6. (D) Ginkgolide A treatment (100 μM) increases the thermal stability of HDAC1 in cell lysates as measured by a temperature-dependent CETSA (n = 4). (E) Ginkgolide A treatment increases the thermal stability of HDAC1 in cell lysates as measured by a concentration-dependent CETSA at 65 °C (n = 4). Data are presented as mean ± SEM.

Data availability

Data will be made available on request.

Acknowledgements

This work was supported by the National Natural Science Foundation of China (Nos. 82173941 and 81774151), Zhejiang Provincial Natural

Science Foundation of China (Grant No. LHDMD22H02001), and the Ministry of Education, Singapore (No. MOE-MOET2EP10120-0007). Y. W. is supported by the Innovation Team and Talents Cultivation Program of the National Administration of Traditional Chinese Medicine (No. ZYYCXTD-D-202002) and Fundamental Research Funds for the Central Universities (No. 226-2023-00114).

Appendix A. Supplementary data

Supplementary data to this article can be found online at <https://doi.org/10.1016/j.bios.2023.115716>.

References

- Arena, G., Casnati, A., Contino, A., Magrì, A., Sansone, F., Sciotto, D., Ungaro, R., 2006. Org. Biomol. Chem. 4, 243–249.
- Arrowsmith, C.H., Bountra, C., Fish, P.V., Lee, K., Schapira, M., 2012. Nat. Rev. Drug. 11, 384–400.
- Attoub, S., Hassan, A.H., Vanhoecke, B., Iratni, R., Takahashi, T., Gaben, A.M., Bracke, M., Awad, S., John, A., Kamalboor, H.A., Al Sultan, M.A., Arafat, K., Gespach, C., Petroianu, G., 2011. Eur. J. Pharmacol. 651, 18–25.
- Baell, J., Walters, M.A., 2014. Nature 513, 481–483.
- Biedermann, F., Schneider, H.J., 2016. Chem. Rev. 116, 5216–5300.
- Choi, M.A., Park, S.Y., Chae, H.Y., Song, Y., Sharma, C., Seo, Y.H., 2019. Sci. Rep. 9, Duvic, M., Talpur, R., Ni, X., Zhang, C., Hazarika, P., Kelly, C., Chiao, J.H., Reilly, J.F., Ricker, J.L., Richon, V.M., Frankel, S.R., 2007. Blood 109, 31–39.
- Falkenberg, K.J., Johnstone, R.W., 2014. Nat. Rev. Drug Discov. 13, 673–691.
- Guo, D.S., Uzunova, V.D., Su, X., Liu, Y., Nau, W.M., 2011. Chem. Sci. 2.
- Ha, M.K., Song, Y.H., Jeong, S.J., Lee, H.J., Jung, J.H., Kim, B., Song, H.S., Huh, J.E., Kim, S.H., 2011. Biol. Pharm. Bull. 34, 1432–1437.
- Hennig, A., Bakirci, H., Nau, W.M., 2007. Nat. Methods 4, 629–632.
- Herr, D.J., Baarine, M., Aune, S.E., Li, X., Ball, L.E., Lemasters, J.J., Beeson, C.C., Chou, J.C., Menick, D.R., 2018. J. Mol. Cell. Cardiol. 114, 309–319.
- Hu, D., Hu, Y., Zhan, T., Zheng, Y., Ran, P., Liu, X., Guo, Z., Wei, W., Wang, S., 2020. Biosens. Bioelectron. 150, 111934.
- Kang, K.A., Piao, M.J., Kim, K.C., Zheng, J., Yao, C.W., Cha, J.W., Kim, H.S., Kim, D.H., Bae, S.C., Hyun, J.W., 2013. Int. J. Oncol. 43, 1907–1914.
- Krämer, O.H., 2023. HDAC/HAT Function Assessment and Inhibitor Development Methods and Protocols, second ed. Springer, New York.
- Li, P., Ge, J., Li, H., 2020. Nat. Rev. Cardiol. 17, 96–115.
- Li, T., Song, B., Wu, Z., Lu, M., Zhu, W.G., 2014. Briefings Bioinf. 15, 963–972.
- Liu, F., Ding, X., Xu, X., Wang, F., Chu, X., Jiang, J.H., 2022. Angew. Chem., Int. Ed. 61, Liu, Q., Wang, J., Boyd, B.J., 2015. Talanta 136, 114–127.
- Liu, X., Xiang, M., Tong, Z., Luo, F., Chen, W., Liu, F., Wang, F., Yu, R.Q., Jiang, J.H., 2018. Anal. Chem. 90, 5534–5539.
- Liu, Y.C., Peng, S., Angelova, L., Nau, W.M., Hennig, A., 2019. ChemistryOpen 8, 1350–1354.
- Lu, L., Li, K., Mao, Y.H., Qu, H., Yao, B., Zhong, W.W., Ma, B., Wang, Z.Y., 2017. Int. J. Oncol. 51, 1089–1103.
- McClure, J.J., Li, X., Chou, C.J., 2018. In: Advances in Cancer Research. Academic Press Inc., pp. 183–211.
- McGovern, R.E., McCarthy, A.A., Crowley, P.B., 2014. Chem. Commun. 50, 10412–10415.
- Molife, L.R., de Bono, J.S., 2011. Expert Opin. Invest. Drugs 20, 1723–1732.
- Moreno-Yruela, C., Bæk, M., Vrsanova, A.E., Schulte, C., Maric, H.M., Olsen, C.A., 2021. Nat. Commun. 12.
- Nalawansha, D.A., Pflum, M.K., 2017. ACS Chem. Biol. 12, 254–264.
- Nau, W.M., Ghale, G., Hennig, A., Bakirci, H., Bailey, D.M., 2009. J. Am. Chem. Soc. 131, 11558–11570.
- Nguyen, B.T., Anslyn, E.V., 2006. Coord. Chem. Rev. 250, 3118–3127.
- Nilam, M., Hennig, A., 2022. RSC Adv. 12, 10725–10748.
- Placzek, E.A., Plebanek, M.P., Lipchik, A.M., Kidd, S.R., Parker, L.L., 2010. Anal. Biochem. 397, 73–78.
- Schwartz, D., Chou, M.F., Church, G.M., 2009. Mol. Cell. Proteomics 8, 365–379.
- Shu, Y., Huang, C., Liu, H., Hu, F., Wen, H., Liu, J., Wang, X., Shan, C., Li, W., 2022. Spectrochim. Acta Mol. Biomol. Spectrosc. 281.
- Singh, A., Chang, T.Y., Kaur, N., Hsu, K.C., Yen, Y., Lin, T.E., Lai, M.J., Lee, S.B., Liou, J.P., 2021. Eur. J. Med. Chem. 215, 113169.
- Singh, T., Prasad, R., Katiyar, S.K., 2013. Epigenetics 8, 54–65.
- Tan, S., Li, X., 2022. Chem Asian J. 17, e202200835.
- Tang, C., Wang, X., Jin, Y., Wang, F., 2022. Biochim. Biophys. Acta Rev. 1877, 188788.
- Umal, A.P., Anslyn, E.V., 2010. Curr. Opin. Chem. Biol. 14, 685–692.
- VanderMolen, K.M., McCulloch, W., Pearce, C.J., Oberlies, N.H., 2011. J. Antibiot. 64, 525–531.
- Wang, D., Li, W., Zhao, R., Chen, L., Liu, N., Tian, Y., Zhao, H., Xie, M., Lu, F., Fang, Q., Liang, W., Yin, F., Li, Z., 2019. Cancer Res. 79, 1769–1783.
- Wang, H., Li, Y., Zhao, K., Chen, S., Wang, Q., Lin, B., Nie, Z., Yao, S., 2017. Biosens. Bioelectron. 91, 400–407.
- Wang, Y., Chen, Y., Wang, H., Cheng, Y., Zhao, X., 2015. Anal. Chem. 87, 5046–5049.
- Wu, W., Li, K., Guo, S., Xu, J., Ma, Q., Li, S., Xu, X., Huang, Z., Zhong, Y., Tettamanti, G., Cao, Y., Li, S., Tian, L., 2021. Cell Death Discovery 7, 128.
- Yang, L., Peltier, R., Zhang, M., Song, D., Huang, H., Chen, G., Chen, Y., Zhou, F., Hao, Q., Bian, L., He, M.L., Wang, Z., Hu, Y., Sun, H., 2020. J. Am. Chem. Soc. 142, 18150–18159.
- You, L., Zha, D., Anslyn, E.V., 2015. Chem. Rev. 115, 7840–7892.
- Yu, H., Chai, X., Geng, W.C., Zhang, L., Ding, F., Guo, D.S., Wang, Y., 2021. Biosens. Bioelectron. 192, 113488.
- Yue, Y.X., Kong, Y., Yang, F., Zheng, Z., Hu, X.Y., Guo, D.S., 2019. ChemistryOpen 8, 1437–1440.
- Zhang, K., Liu, Z., Yao, Y., Qiu, Y., Li, F., Chen, D., Hamilton, D.J., Li, Z., Jiang, S., 2021. J. Med. Chem. 64, 4020–4033.
- Zhao, Y., Zou, J., Song, Y., Peng, J., Wang, Y., Bi, Y., 2020. Chem. Commun. 56, 1629–1632.
- Zheng, Z., Geng, W.C., Li, H. Bin, Guo, D.S., 2021. Supramol. Chem. 33, 80–87.